JCB Report

H2AX regulates meiotic telomere clustering

Oscar Fernandez-Capetillo,[1] Bodo Liebe,[2] Harry Scherthan,[2] and André Nussenzweig[1]

[1]Experimental Immunology Branch, National Cancer Institute, National Institutes of Health, Bethesda, MD 20892
[2]Max-Planck-Institut für Molekulare Genetik, D-14195 Berlin, Germany

The histone H2A variant H2AX is phosphorylated in response to DNA double-strand breaks originating from diverse origins, including dysfunctional telomeres. Here, we show that normal mitotic telomere maintenance does not require H2AX. Moreover, *H2AX* is dispensable for the chromosome fusions arising from either critically shortened or deprotected telomeres. However, H2AX has an essential role in controlling the proper topological distribution of telomeres during meiotic prophase I. Our results suggest that H2AX is a downstream effector of the ataxia telangiectasia–mutated kinase in controlling telomere movement during meiosis.

Introduction

Telomeres are not only critical components of somatic chromosomes, but also play a unique function during meiosis. Meiosis is a cellular differentiation program during which physiological double-strand breaks (DSBs) are created and repaired, giving rise to recombination events between parental chromosomes. During the first meiotic prophase, telomeres redistribute and cluster, forming a so-called "bouquet," which may ensure proper homologue pairing before recombination (Loidl, 1990; Scherthan, 2001; Yamamoto and Hiraoka, 2001). The ataxia telangiectasia–mutated (ATM) kinase is required for transit through early prophase I (Pandita, 2002). In addition, ATM disruption has been found to alter telomere dynamics, leading to an accumulation of bouquet-stage nuclei with perturbed synapsis during zygotene (Pandita et al., 1999; Scherthan et al., 2000).

One of the immediate targets of the ATM kinase in response to DNA damage is the histone H2A variant H2AX (Redon et al., 2002). The analysis of *H2AX*-deficient mice has demonstrated a role for *H2AX* in a variety of responses to DSBs, including DNA repair, checkpoint signaling, and Ig class switching (Petersen et al., 2001; Bassing et al., 2002; Celeste et al., 2002; Fernandez-Capetillo et al., 2002; Reina-San-Martin et al., 2003). Similar to *ATM*-deficient cells, $H2AX^{-/-}$ cells senesce within a few passages in culture, and display an increased frequency of chromosomal aberrations (Celeste et al., 2002, 2003a). Moreover, $H2AX^{-/-}$ mice exhibit male-specific sterility, which is likely due to defects in chromatin remodeling during meiosis (Fernandez-Capetillo et al., 2003). Because of the strong correlation between defective DSB repair, genomic instability, and telomere dysfunction, we examined the role of H2AX in both mitotic and meiotic telomere maintenance.

Results and discussion

To determine whether H2AX regulates telomere length, we performed quantitative FISH (Zijlmans et al., 1997) on metaphase spreads derived from four independent sets of *H2AX* knockout and control mouse embryonic fibroblasts (MEFs). Although telomeres were slightly elongated in some of the $H2AX^{-/-}$ MEFs relative to $H2AX^{+/+}$ isogenic cultures (Table I), this difference in telomere length was not statistically significant (t test, $P > 0.1$; at least 15 metaphases examined for each culture). Moreover, both genotypes displayed a similar heterogeneity in the frequency of telomere fluorescence intensities, indicating that H2AX deficiency did not modify the distribution of individual telomere lengths (Fig. S1, available at http://www.jcb.org/cgi/content/full/jcb.200305124/DC1). To rule out the possibility that the decreased proliferative capacity of $H2AX^{-/-}$ MEFs (Celeste et al., 2002) could bias the measurements of telomere lengths, we performed quantitative FISH in a variety of other primary cells including splenocytes, purified B cells, and lymph node T cells, derived from independent $H2AX^{+/+}$ and $H2AX^{-/-}$ littermates (Table S1). None of the cell types showed a significant difference in telomere length (t test, $P > 0.1$; at least 15 metaphases examined for each culture).

The online version of this article includes supplemental material.

Address correspondence to André Nussenzweig, Experimental Immunology Branch, National Cancer Institute, National Institutes of Health, Bethesda, MD 20892. Tel.: (301) 435-6425. Fax: (301) 496-0887. email: andre_nussenzweig@nih.gov

Key words: DNA repair; genomic instability; meiosis; ATM; spermatocyte

Abbreviations used in this paper: ATM, ataxia telangiectasia mutated; DSB, double-strand break; MEF, mouse embryonic fibroblast; SC, synaptonemal complex; Terc, RNA component of telomerase.

Table I. **Quantitative FISH analysis of telomere length**

Litter	Genotype[a]	Chromosome arm	Telomere length [A.U. (SD)]
A	+/+	p	1285 (352)
		q	1509 (429)
		Total	1397 (389)
	−/−	p	1365 (368)
		q	1661 (492)
		Total	1513 (423)
B	+/+	p	1320 (356)
		q	1550 (421)
		Total	1435 (386)
	−/−	p	1206 (339)
		q	1506 (461)
		Total	1356 (412)
	+/+	p	1335 (377)
		q	1601 (546)
		Total	1468 (476)
	−/−	p	1465 (479)
		q	1687 (526)
		Total	1576 (503)
C	+/+	p	1469 (571)
		q	1699 (658)
		Total	1584 (624)
	−/−	p	1457 (568)
		q	1807 (695)
		Total	1632 (631)

+/+, $H2AX^{+/+}$; −/−, $H2AX^{-/-}$. A.U., arbitrary units; SD, standard deviation.
[a]At least 15 metaphases were used per analyzed cell culture.

As an additional quantitative measurement, we analyzed telomere lengths in B and T lymphocytes by flow cytometry FISH (Rufer et al., 1998), which confirmed the lack of significant differences between the two genotypes (unpublished data). We conclude that H2AX does not regulate telomere length in mice.

H2AX deficiency is associated with chromosomal instability (Bassing et al., 2002, 2003; Celeste et al., 2002, 2003a). To determine whether chromosomal aberrations arise in part from modifications in telomere structure, as is the case in numerous mouse models with defects in DSB repair (Goytisolo and Blasco, 2002), we analyzed individual metaphase spreads from four $H2AX^{+/+}$ and $H2AX^{-/-}$ MEF cell lines that had been subjected to telomere FISH. Consistent with our previous observations (Celeste et al., 2002), $H2AX^{-/-}$ MEFs exhibited a dramatic increase in chromosome breaks relative to wild-type controls (Fig. 1 A, bottom; Fig. 1 C). However, despite the high level of genomic instability in $H2AX^{-/-}$ cells, we did not detect any significant increase in the number of telomere fusions in these cells (Fig. 1 A, top). Thus, telomere dysfunction does not contribute significantly to the increased genomic instability in $H2AX^{-/-}$ mice.

To further examine the impact of H2AX deficiency on chromosomal instability in the presence of shortened telomeres, we intercrossed $H2AX^{+/-}$ mice with successive generations of mice deficient in the RNA component of telomerase (Terc; Blasco et al., 1997; Fig. S2, available at http://www.jcb.org/cgi/content/full/jcb.200305124/DC1). Consistent with previous reports (Lee et al., 1998; Hande et al., 1999), we observed a dramatic increase in the percentage of telomere fusions arising in successive generations of $Terc^{-/-}$ mice (Fig. 1 A, top; Fig. 1 C). However, H2AX deficiency had no apparent role in this type of fusion because a similar percentage of telomere fusions was observed in four independent G5 $H2AX^{-/-}Terc^{-/-}$ (6 ± 2.1%) and G5 $H2AX^{+/+}Terc^{-/-}$ (5.9 ± 1.6%) MEF cultures. Although $H2AX^{-/-}$ MEFs exhibited slightly higher levels of chromosome breaks in the late generation *Terc* knockout background than in the presence of Terc (Fig. 1 A, bottom), this difference was not statistically significant (G0 $H2AX^{-/-}$ vs. G5 $H2AX^{-/-}$; *t* test, $P > 0.1$). This finding is in contrast to ATM deficiency, which has been shown to exacerbate telomere fusions and instability in the absence of *Terc* (Wong et al., 2003).

Telomere fusions not only arise from shortened telomeres, but also arise from structural alterations such as those triggered by the inactivation of telomere-associated proteins. For example, inhibition of TRF2 results in end–end fusions, which are generated by the nonhomologous end-joining (NHEJ) DNA repair pathway (Smogorzewska et al., 2002). Recent reports documented the association of several DNA damage response factors—including γ-H2AX—at uncapped telomeres (d'Adda di Fagagna et al., 2003; Takai et al., 2003). To determine the role of H2AX in fusions arising from deprotected telomeres, $H2AX^{+/+}$ and $H2AX^{-/-}$ MEFs were infected with a TRF2 dominant-negative–expressing retrovirus ($TRF2^{\Delta B\Delta M}$) or with the corresponding vector pLPC (Karlseder et al., 1999). Following the strategy used to assess the role of the NHEJ factor DNA ligase IV in telomere fusions (Smogorzewska et al., 2002), MEFs were generated in a p53-deficient background, which partially alleviates the growth defects in primary $H2AX^{-/-}$ MEFs (Celeste et al., 2002, 2003a). In contrast to DNA ligase IV, H2AX was not essential for fusions arising from TRF2 dominant-negative infection (Fig. 1, B and C). In 30 metaphases examined by telomere FISH, we observed a total of 43 telomere fusions in $H2AX^{-/-}p53^{-/-}$ MEFs, compared with 29 fusions in $H2AX^{+/+}p53^{-/-}$ MEFs. Thus, although H2AX appears to modulate NHEJ (Downs et al., 2000; Bassing et al., 2003; Celeste et al., 2003a), H2AX is not required for chromosome fusions arising from either shortened or structurally deprotected telomeres.

During mouse meiosis, telomeres reposition along the nuclear periphery to create a characteristic bouquet configuration. This clustering of chromosome ends generally occurs at the leptotene/zygotene transition (Scherthan, 2001), coincident with the initiation of homologous DSB repair (for review see Hunter et al., 2001). To date, the only protein that has been implicated in the regulation of the bouquet stage in mammals is the ATM kinase (Pandita et al., 1999). To determine whether the ATM target H2AX is involved in meiotic telomere dynamics, we investigated telomere and centromere behavior by FISH (Scherthan et al., 1996) in wild-type and H2AX-deficient testes preparations from 4-wk-old mice (Fig. 2 A). The analysis of structurally preserved spermatocyte nuclei revealed similar frequencies of preleptotene spermatocytes (1.0 vs. 1.6%) in wild-type and mutant testes suspensions (based on 2,772 wild-type and 2,567 mutant nuclei), respectively, with the difference

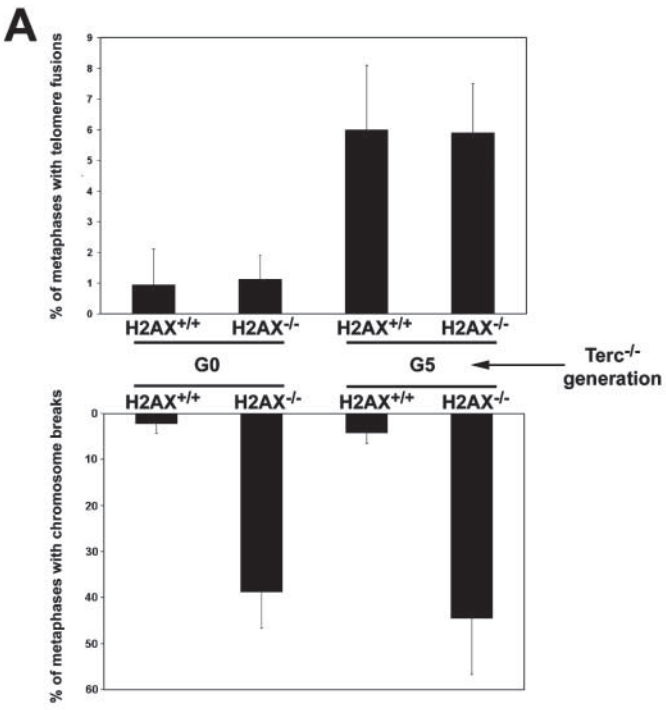

B

Chromosomal Aberrations in 30 Metaphase Cells

Genotype/Retrovirus	Fusions with Telomeric Signal	Fusions without Telomeric Signal	Breaks and Fragments
$H2AX^{+/+}$ $p53^{-/-}$/vector	3	2	8
$H2AX^{+/+}$ $p53^{-/-}$/$TRF2^{\Delta B\Delta M}$	29	1	15
$H2AX^{-/-}$ $p53^{-/-}$/vector	7	3	42
$H2AX^{-/-}$ $p53^{-/-}$/$TRF2^{\Delta B\Delta M}$	43	2	49

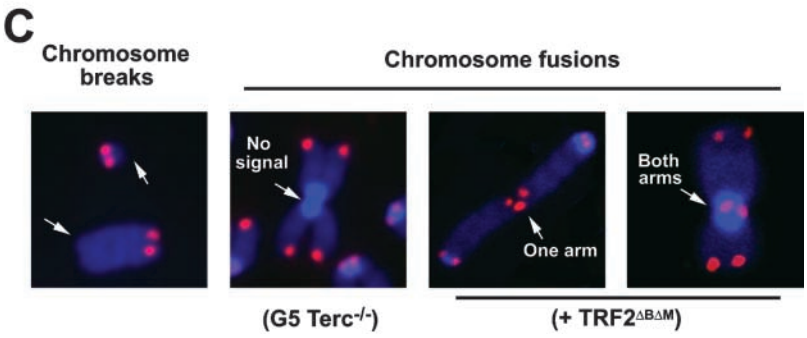

Figure 1. **Normal telomere maintenance in *H2AX*-deficient somatic cells.** (A) Frequency of telomere fusions (top) and chromosome breaks (bottom) in metaphases from late generation (G5) $Terc^{-/-}$ MEFs in $H2AX^{+/+}$ or $H2AX^{-/-}$ backgrounds compared with those found in wild-type ($H2AX^{+/+}Terc^{+/+}$) or H2AX-deficient ($H2AX^{-/-}Terc^{+/+}$) MEFs (G0). All metaphases were derived from four independent pairs of littermate MEFs at passage 3, and the number of metaphases examined for each MEF ranged from 68 to 126. The frequency of metaphases containing each type of aberration is plotted. (B) Summary of chromosomal abnormalities found in $H2AX^{+/+}p53^{-/-}$ and $H2AX^{-/-}p53^{-/-}$ MEFs that had been infected with pLPC-$TRF2^{\Delta B\Delta M}$–expressing retrovirus (or control virus pLPC). (C) Examples of chromosomal aberrations found in $H2AX^{-/-}$ MEFs (red, telomeric DNA; blue, DAPI).

being statistically insignificant ($P = 0.1$; χ^2 and Fisher test; Fig. 2 B). However, we noted a 20-fold increase in the frequency of $H2AX^{-/-}$ bouquet-stage nuclei ($H2AX^{-/-}$, 6%; wild-type, 0.4%; based on 2,567 mutant and 2,772 wild-type spermatogenic nuclei), with the differences being highly significant ($P < 0.0001$; χ^2 and Fisher test; Fig. 2 B). To determine the stages in which elevated levels of bouquet nuclei accumulate, we combined immunostaining of the telomere-associated protein TRF1 with that of SCP3 (Lammers et al., 1994), a component of the axial/lateral element of the synaptonemal complex (SC; Fig. 2 C). Three-dimensional microscopy revealed that TRF1 signals capped the ends of axial/lateral elements that clustered at the nuclear envelope. Strikingly, many of the structurally preserved $H2AX^{-/-}$ prophase I nuclei displayed a bouquet topology with telomeres clustered in a limited nuclear envelope region from early leptotene until early pachytene, with long U-shaped SCs emanating from the clustered telomeres (Fig. 2 C). The occurrence of telomere clustering as early as leptotene and its maintenance up to late zygotene/pachytene stages contrasts with wild-type spermatogenesis of adult mice, where telomere clustering occurs only in a limited time window during the leptotene/zygotene transition (Scherthan et al., 1996). In testes suspensions of wild-type mice, bouquet-stage cells are generally detected at an average frequency of 0.2–0.8%, which underlines the short-lived nature of this stage in spermatogenesis (Scherthan et al., 1996, 2000). Thus, the significant increase in bouquet

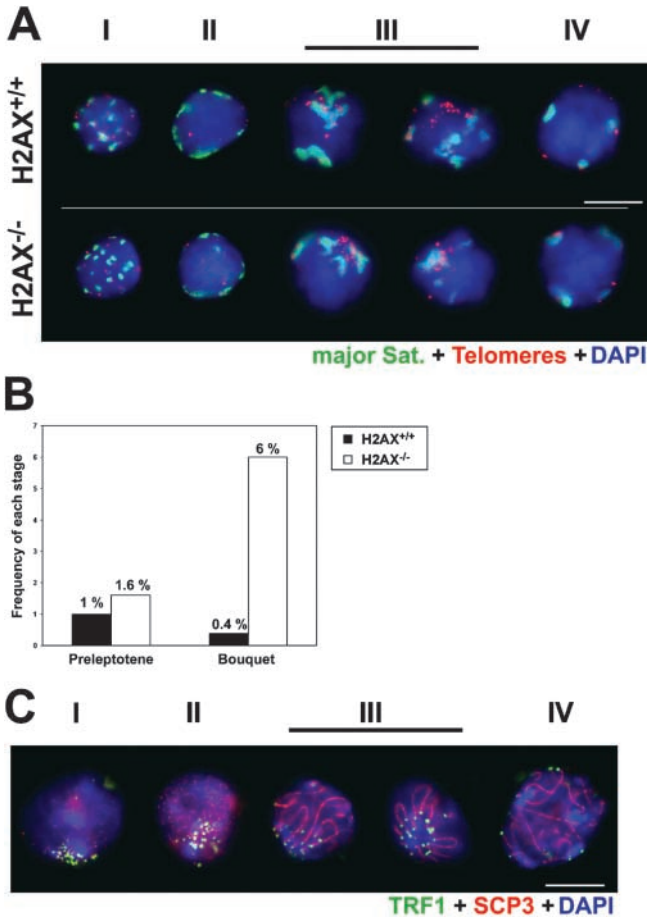

Figure 2. ***H2AX* inactivation results in aberrant telomere clustering during meiotic prophase I.** (A) Telomere (red)–centromere (green) FISH patterns in structurally preserved spermatocytes. (I) Premeiotic nuclei with numerous internal telomere and satellite DNA clusters (focal plane at nuclear equator). (II) Preleptotene nuclei with peripheral satellite DNA clusters. (III) Two bouquet nuclei each with clustered telomeres (leptotene/zygotene; focal plane at nuclear top). (IV) Pachytene nuclei with dispersed peripheral telomeres and satellite DNA clusters (focal plane at nuclear equator). (B) Frequency of preleptotene and bouquet spermatocytes, with the latter being dramatically increased in the *H2AX* knockout; see Results for details. (C) Immunofluorescence of axial/lateral cores (SCP3, red) and telomeres (TRF1, green) in structurally preserved $H2AX^{-/-}$ nuclei (DAPI, blue). (I) Early leptotene nucleus with a tight telomere cluster at a sector of the nuclear periphery and SCP3 speckles. (II) More advanced leptotene with short SCP3 threads and clustered telomeres. (III) Two late zygotene/pachytene bouquet nuclei with more relaxed telomere clustering near the nuclear top and U-shaped SCs that extend into the nuclear lumen. (IV) Pachytene nucleus with meandering SCs and telomeres dispersed around the nuclear periphery. Bar, 10 μm.

frequencies in the *H2AX* knockouts as compared with age-matched controls suggests that the absence of *H2AX* leads to an extended bouquet stage. Moreover, in contrast to wild-type spermatocytes, which exhibit massive H2AX phosphorylation in response to Spo11-mediated DSBs (Mahadevaiah et al., 2001), we found that γ-H2AX staining was largely absent in $ATM^{-/-}$ leptotene/zygotene-stage spermatocytes (Fig. S3, available at http://www.jcb.org/cgi/content/full/jcb.200305124/DC1), therefore demonstrating that meiotic DSB-triggered γ-H2AX formation is dependent on ATM. These results place H2AX downstream of ATM in the signal transduction pathway that orchestrates meiotic telomere clustering.

The initiation of telomere clustering appears to be a default reaction because it occurs in the absence of synapsis, homologous chromosomes, and/or recombination (for review see Scherthan, 2001). However, the accumulation of bouquet-stage meiocytes in DSB and SC-deficient yeast or worm meiosis (Trelles-Sticken et al., 1999; MacQueen et al., 2002) suggests that the resolution of telomere clustering is triggered upon completion of synapsis and/or repair. Consistent with this, both $H2AX^{-/-}$ and $ATM^{-/-}$ mice display an accumulation of spermatocytes with persistence of bouquet topology. The fact that bouquet-type arrangements in *H2AX*-deficient spermatocytes are observable up to pachytene suggests that the increased telomere clustering observed in *ATM*-deficient cells may be directly related to impaired phosphorylation of H2AX, rather than being an indirect consequence of the early leptotene/zygotene arrest. According to this view, ATM facilitates telomere-promoted homologue pairing via phosphorylation of H2AX, thereby coordinating clustering with the initiation of DSB repair. The dissolution of meiotic telomere clustering would then depend on the dephosphorylation of γ-H2AX, which may signal the completion of DSB repair and/or induce changes in higher order chromatin structure (Fernandez-Capetillo et al., 2003). Because the exit from the bouquet stage is coordinated with completion of DSB repair (Trelles-Sticken et al., 1999; MacQueen et al., 2002), the elevated telomere clustering in $H2AX^{-/-}$ spermatocytes may therefore reflect an altered repair capacity of the H2AX knockout spermatocytes.

Like many other mouse models with defects in DSB repair and/or telomere maintenance, absence of H2AX is associated with growth defects, radiation sensitivity, genomic instability, and cancer predisposition (Bassing et al., 2002, 2003; Celeste et al., 2002, 2003a). Although a number of DNA repair proteins play essential roles in maintaining telomere structure, we have found that H2AX is largely dispensable for somatic telomere maintenance. In principle, this could be explained by the fact that H2AX is not required for the recruitment of damage sensors to DNA lesions, and therefore, the cellular response to unprotected chromosome ends may proceed normally in its absence (Celeste et al., 2003b). However, H2AX is essential for the proper spatial rearrangement of chromosome ends during the first meiotic prophase. Further analysis will be necessary to dissect the role of meiotic telomer clustering and its dissolution with respect to homologue pairing and DSB repair.

Materials and methods

Mice and cell lines

Generation of $H2AX^{-/-}$, $ATM^{-/-}$, and $Terc^{-/-}$ mice have been described previously (Barlow et al., 1996; Blasco et al., 1997; Celeste et al., 2002). E13.5 MEFs were obtained from intercrossing mice following standard procedures, and $H2AX^{-/-}p53^{-/-}$ MEFs are described elsewhere (Celeste et al., 2003a). For all experiments, littermates were compared. B lymphocytes were isolated using CD19 microbeads (Miltenyi Biotec), and were stimulated with LPS or LPS+IL4 as described previously (Celeste et al., 2002). Splenocytes or lymph node–derived B and T lymphocytes were stimulated with either LPS or Con A, respectively.

Analysis of telomere lengths and fusions

Quantitative FISH analysis using a Cy3-labeled (CCCTAA) peptide nucleic acid probe (Applied Biosystems) was performed as described previously (Zijlmans et al., 1997; Hande et al., 1999). Telomere length measurements were performed on least 15 metaphases for each cell type. DAPI chromosome and Cy3 telomere images were acquired with a constant exposure time that ensured all captured fluorescent signals were within the linear range. All the images from matched littermate samples were acquired blindly and in parallel on the same day. To correct for differences in the microscope settings and hybridization efficiencies, the fluorescence intensity of Cy3-labeled fluorescent beads (Molecular Probes, Inc.) was used to normalize intensities from different experiments. Quantitative analysis of telomere fluorescence was performed with the TFL Telo software, which allows for a proper identification and editing of individual telomere intensities (a gift from Dr. Peter Lansdorp). Statistical analysis of the measured telomere intensities was performed with Microsoft® Excel 2000 (Microsoft Corp.) and Prophet (BBN Technologies) softwares. Chromosomal aberrations, including breaks and telomere fusions, were scored by examining DAPI and telomeric images from at least 65 metaphases derived from cultures of $H2AX^{+/+}Terc^{+/+}$ (G0), $H2AX^{-/-}Terc^{+/+}$ (G0), $H2AX^{+/+}Terc^{-/-}$ (G5), and $H2AX^{-/-}Terc^{-/-}$ (G5) MEFs (a total of 417, 355, 357, and 346 metaphases were examined, respectively, for each genotype).

Retroviral infection and plasmids

pLPC-puro and pLPC-TRF2$^{\Delta B\Delta M}$ retroviral vectors have been described previously (Karlseder et al., 1999). For retroviral infection, Phoenix α cells (American Type Culture Collection) were seeded at 5×10^6 cells/10-cm dish, and 20 μg of each plasmid was transfected using $CaPO_4$. 5 h after transfection, the cells were washed with PBS and the medium was replenished. A 10-ml supernatant was collected 72 h after transfection, passed through a 0.45-μm filter, and supplemented with polybrene at 4 μg/ml. MEFs were seeded 24 h before infection at 8×10^5 cells/10-cm dish. For infection, MEFs were overlaid with virus-containing medium, and centrifuged for 1.5 h at 1,500 rpm. Cells were split into three 10-cm dishes 24 h after infection, and the medium was replaced by DME/15% FCS containing 2 μg puromycin per ml. Metaphases were prepared 96 h after selection.

Testicular preparations and bouquet analysis

Testes suspensions containing structurally preserved nuclei for simultaneous SC immunostaining, FISH, and bouquet analysis were prepared and analyzed as described previously (Scherthan et al., 2000; Scherthan, 2002). Preleptotene and bouquet nuclei were identified by perinuclear major satellite DNA or telomeres clustered at a limited sector of the nuclear periphery, respectively (Scherthan et al., 1996).

Online supplemental material

Fig. S1 demonstrates similar frequency distribution of telomere fluorescence in H2AX$^{+/+}$ vs. H2AX$^{-/-}$ MEFs. Fig. S2 is a schematic representation of the generation of H2AX$^{-/-}$Terc$^{-/-}$ mice with progressively shortened telomeres. Fig. S3 demonstrates ATM-dependent phosphorylation of H2AX in response to meiotic double-strand breaks. Online supplemental material available at http://www.jcb.org/cgi/content/full/jcb.200305124/DC1.

We thank P. Lansdorp and S.S. Poon for providing the TFL Telo image analysis program; T. de Lange for providing the retroviral constructs and TRF1 antibodies; and Dr. Richard Hodes for critical comments on the manuscript. H. Scherthan thanks T. de Lange (The Rockefeller University, New York, NY) and C. Heyting (Wageningen University, Wageningen, Netherlands) for providing SCP3 antibodies.

H. Scherthan acknowledges support from the Deutsche Forschungsgemeinschaft (HS350/8-4).

Submitted: 27 May 2003
Accepted: 5 September 2003

References

Barlow, C., S. Hirotsune, R. Paylor, M. Liyanage, M. Eckhaus, F. Collins, Y. Shiloh, J.N. Crawley, T. Ried, D. Tagle, and A. Wynshaw-Boris. 1996. Atm-deficient mice: a paradigm of ataxia telangiectasia. *Cell.* 86:159–171.

Bassing, C.H., K.F. Chua, J. Sekiguchi, H. Suh, S.R. Whitlow, J.C. Fleming, B.C. Monroe, D.N. Ciccone, C. Yan, K. Vlasakova, et al. 2002. Increased ionizing radiation sensitivity and genomic instability in the absence of histone H2AX. *Proc. Natl. Acad. Sci. USA.* 99:8173–8178.

Bassing, C.H., H. Suh, D.O. Ferguson, K.F. Chua, J. Manis, M. Eckersdorff, M. Gleason, R. Bronson, C. Lee, and F.W. Alt. 2003. Histone H2AX. A dosage-dependent suppressor of oncogenic translocations and tumors. *Cell.* 114: 359–370.

Blasco, M.A., H.W. Lee, M.P. Hande, E. Samper, P.M. Lansdorp, R.A. DePinho, and C.W. Greider. 1997. Telomere shortening and tumor formation by mouse cells lacking telomerase RNA. *Cell.* 91:25–34.

Celeste, A., S. Petersen, P.J. Romanienko, O. Fernandez-Capetillo, H.T. Chen, O.A. Sedelnikova, B. Reina-San-Martin, V. Coppola, E. Meffre, M.J. Difilippantonio, et al. 2002. Genomic instability in mice lacking histone H2AX. *Science.* 296:922–927.

Celeste, A., S. Difilippantonio, M.J. Difilippantonio, O. Fernandez-Capetillo, D.R. Pilch, O.A. Sedelnikova, M. Eckhaus, T. Ried, W.M. Bonner, and A. Nussenzweig. 2003a. H2AX haploin sufficiency modifies genomic stability and tumor susceptibility. *Cell.* 114:371–383.

Celeste, A., O. Fernandez-Capetillo, M.J. Kruhlak, D.R. Pilch, D.W. Staudt, A. Lee, R.F. Bonner, W.M. Bonner, and A. Nussenzweig. 2003b. Histone H2AX phosphorylation is dispensable for the initial recognition of DNA breaks. *Nat. Cell Biol.* 5:675–679.

d'Adda di Fagagna, F., P.M. Reaper, L. Clay-Farrace, H. Fiegler, P.Carr, T. von Zglinicki, G. Saretzk, N.P. Carter, and S.P. Jackson. 2003. A DNA damage checkpoint-mediated response in telomere-initiated cellular senescence. *Nature*. In press.

Downs, J.A., N.F. Lowndes, and S.P. Jackson. 2000. A role for *Saccharomyces cerevisiae* histone H2A in DNA repair. *Nature.* 408:1001–1004.

Fernandez-Capetillo, O., H.T. Chen, A. Celeste, I. Ward, P.J. Romanienko, J.C. Morales, K. Naka, Z. Xia, R.D. Camerini-Otero, N. Motoyama, et al. 2002. DNA damage-induced G2-M checkpoint activation by histone H2AX and 53BP1. *Nat. Cell Biol.* 4:993–997.

Fernandez-Capetillo, O., S.K. Mahadevaiah, A. Celeste, P.J. Romanienko, R.D. Camerini-Otero, W.M. Bonner, K. Manova, P. Burgoyne, and A. Nussenzweig. 2003. H2AX is required for chromatin remodeling and inactivation of sex chromosomes in male mouse meiosis. *Dev. Cell.* 4:497–508.

Goytisolo, F.A., and M.A. Blasco. 2002. Many ways to telomere dysfunction: in vivo studies using mouse models. *Oncogene.* 21:584–591.

Hande, M.P., E. Samper, P. Lansdorp, and M.A. Blasco. 1999. Telomere length dynamics and chromosomal instability in cells derived from telomerase-null mice. *J. Cell Biol.* 144:589–601.

Hunter, N., G. Valentin Borner, M. Lichten, and N. Kleckner. 2001. Gamma-H2AX illuminates meiosis. *Nat. Genet.* 27:236–238.

Karlseder, J., D. Broccoli, Y. Dai, S. Hardy, and T. de Lange. 1999. p53- and ATM-dependent apoptosis induced by telomeres lacking TRF2. *Science.* 283:1321–1325.

Lammers, J.H., H.H. Offenberg, M. van Aalderen, A.C. Vink, A.J. Dietrich, and C. Heyting. 1994. The gene encoding a major component of the lateral elements of synaptonemal complexes of the rat is related to X-linked lymphocyte-regulated genes. *Mol. Cell. Biol.* 14:1137–1146.

Lee, H.W., M.A. Blasco, G.J. Gottlieb, J.W. Horner, II, C.W. Greider, and R.A. DePinho. 1998. Essential role of mouse telomerase in highly proliferative organs. *Nature.* 392:569–574.

Loidl, J. 1990. The initiation of meiotic chromosome pairing: the cytological view. *Genome.* 33:759–778.

MacQueen, A.J., M.P. Colaiacovo, K. McDonald, and A.M. Villeneuve. 2002. Synapsis-dependent and -independent mechanisms stabilize homolog pairing during meiotic prophase in *C. elegans*. *Genes Dev.* 16:2428–2442.

Mahadevaiah, S.K., J.M. Turner, F. Baudat, E.P. Rogakou, P. de Boer, J. Blanco-Rodriguez, M. Jasin, S. Keeney, W.M. Bonner, and P.S. Burgoyne. 2001. Recombinational DNA double-strand breaks in mice precede synapsis. *Nat. Genet.* 27:271–276.

Pandita, T.K. 2002. ATM function and telomere stability. *Oncogene.* 21:611–618.

Pandita, T.K., C.H. Westphal, M. Anger, S.G. Sawant, C.R. Geard, R.K. Pandita, and H. Scherthan. 1999. Atm inactivation results in aberrant telomere clustering during meiotic prophase. *Mol. Cell. Biol.* 19:5096–5105.

Petersen, S., R. Casellas, B. Reina-San-Martin, H.T. Chen, M.J. Difilippantonio, P.C. Wilson, L. Hanitsch, A. Celeste, M. Muramatsu, D.R. Pilch, et al. 2001. AID is required to initiate Nbs1/gamma-H2AX focus formation and mutations at sites of class switching. *Nature.* 414:660–665.

Redon, C., D. Pilch, E. Rogakou, O. Sedelnikova, K. Newrock, and W. Bonner. 2002. Histone H2A variants H2AX and H2AZ. *Curr. Opin. Genet. Dev.* 12: 162–169.

Reina-San-Martin, B., S. Difilippantonio, L. Hanitsch, R.F. Masilamani, A. Nussenzweig, and M.C. Nussenzweig. 2003. H2AX is required for recombina-

tion between immunoglobulin switch regions but not for intra-switch region recombination or somatic hypermutation. *J. Exp. Med.* 197:1767–1778.

Rufer, N., W. Dragowska, G. Thornbury, E. Roosnek, and P.M. Lansdorp. 1998. Telomere length dynamics in human lymphocyte subpopulations measured by flow cytometry. *Nat. Biotechnol.* 16:743–747.

Scherthan, H. 2001. A bouquet makes ends meet. *Nat. Rev. Mol. Cell Biol.* 2:621–627.

Scherthan, H. 2002. Detection of chromosome ends by telomere FISH. *Methods Mol. Biol.* 191:13–31.

Scherthan, H., S. Weich, H. Schwegler, C. Heyting, M. Harle, and T. Cremer. 1996. Centromere and telomere movements during early meiotic prophase of mouse and man are associated with the onset of chromosome pairing. *J. Cell Biol.* 134:1109–1125.

Scherthan, H., M. Jerratsch, S. Dhar, Y.A. Wang, S.P. Goff, and T.K. Pandita. 2000. Meiotic telomere distribution and Sertoli cell nuclear architecture are altered in Atm- and Atm-p53-deficient mice. *Mol. Cell. Biol.* 20:7773–7783.

Smogorzewska, A., J. Karlseder, H. Holtgreve-Grez, A. Jauch, and T. de Lange. 2002. DNA ligase IV-dependent NHEJ of deprotected mammalian telomeres in G1 and G2. *Curr. Biol.* 12:1635–1644.

Takai, T., A. Smogorzewska, and T. de Lange. 2003. DNA damage foci at dysfunctional telomeres. *Curr. Biol.* 13:1549–1556. First published on July 23, 2003; 10.1016/S0960982203005426.

Trelles-Sticken, E., J. Loidl, and H. Scherthan. 1999. Bouquet formation in budding yeast: initiation of recombination is not required for meiotic telomere clustering. *J. Cell Sci.* 112:651–658.

Wong, K.K., R.S. Maser, R.M. Bachoo, J. Menon, D.R. Carrasco, Y. Gu, F.W. Alt, and R.A. DePinho. 2003. Telomere dysfunction and Atm deficiency compromises organ homeostasis and accelerates ageing. *Nature.* 421:643–648.

Yamamoto, A., and Y. Hiraoka. 2001. How do meiotic chromosomes meet their homologous partners?: lessons from fission yeast. *Bioessays.* 23:526–533.

Zijlmans, J.M., U.M. Martens, S.S. Poon, A.K. Raap, H.J. Tanke, R.K. Ward, and P.M. Lansdorp. 1997. Telomeres in the mouse have large inter-chromosomal variations in the number of T2AG3 repeats. *Proc. Natl. Acad. Sci. USA.* 94:7423–7428.